Research Article

Benjamin M. Kurtz*, Demián D. Gómez, and Michael G. Bevis

Characterization of the precision of PPP solutions as a function of latitude and session length

https://doi.org/10.1515/jogs-2022-0176
received March 28, 2024; accepted June 28, 2024

Abstract: This study investigates the impact of observation session duration and station latitude on the precision of Precise Point Positioning (PPP). Global Positioning System-only Receiver Independent Exchange files from 516 continuous stations spanning latitudes from 90°N to 90°S across the Americas (30°–130°W) were binned into sessions of 1, 2, 3, 4, 6, and 12 h and processed using the GPSPACE PPP software. These sub-daily solutions, along with the original 24 h ones, were compared against a reference coordinate derived from an extended linear trajectory model for each station. Analysis of the results, considering both accuracy and precision, was conducted across the entire latitude range of the study. We found that the precision of a PPP solution approximately follows a power-law relationship with observation duration. Parameters for these power-law relationships were determined for all latitude ranges that allow users to predict a result's uncertainty as a function of session length. Findings indicate that longer observation sessions lead to reduced positioning errors, with vertical scatter *decreasing* with increasing latitude. Since all these stations are characterized by good to excellent sky view, our power-law rule-of-thumb provides a lower bound on the occupation time needed to achieve target positioning precision at locations with poorer sky visibility.

Keywords: Global Positioning System, Parallel.GAMIT, precise point positioning, short observation duration

*** Corresponding author: Benjamin M. Kurtz,** Division of Geodetic Science, School of Earth Sciences, The Ohio State University, Columbus, Ohio, United States of America, e-mail: kurtz.359@osu.edu
Demián D. Gómez, Michael G. Bevis: Division of Geodetic Science, School of Earth Sciences, The Ohio State University, Columbus, Ohio, United States of America

1 Introduction

Global Navigation Satellite Systems (GNSS) Precise Point Positioning (PPP; Zumberge et al., 1997) is a data processing technique that calculates absolute coordinates in the orbital reference frame with millimeter-level precision (Kouba et al., 2017) using pseudo-range and carrier phase measurements from a single, double-frequency GNSS receiver. Unlike the double differences (DD) positioning technique, PPP relies on precise satellite orbits and clock products to mitigate errors in GNSS signals (Kouba and Héroux, 2001).

In recent decades, PPP has gained popularity in surveying applications as an alternative to the relative positioning technique, especially in areas lacking geodetic infrastructure. This surge in popularity is attributed to the advantages over relative positioning because it reduces labor and logistics costs as it doesn't require the use of local base stations, and the loss of accuracy associated with PPP is now relatively minor. Moreover, the system of equations necessary to solve for a PPP coordinate is simpler than that of a DD solution, and therefore, the computational power needed for PPP is much lower compared to DD.

Although PPP offers these advantages, there are some disadvantages related to the minimum duration of an observation session. Users typically need to collect data for at least 15 min to a few hours to resolve initial phase ambiguities and obtain a precise position solution (Kouba et al., 2017). Furthermore, although ultra-rapid and rapid satellite products exist, users requiring high-precision solutions need to wait for precise satellite orbital products in order to achieve millimeter-level precision. Hence, real-time PPP applications have limited precision compared to short- or medium-baseline (up to ~100 km) DD solutions.

Several studies have been conducted on the understanding of PPP solutions' scatter across various sub-daily durations relative to a 24-h session. Previous investigations focused on comparing PPP (using various software) with relative positioning, exploring ambiguity resolution effects on station parameters (position, tropospheric delay, etc.), and assessing the impact of incorporating observations from multiple GNSS constellations. For example, Ghoddousi-Fard and

Dare (2006) presented an analysis of GNSS online processing services. Although their data set was rather limited, the study concluded that a 10-h session can achieve results comparable to those obtained using a 24-h observation session. Tsakiri (2008) indicated repeatable solutions at the 1–2 cm level for 24-h files and decreasing accuracy for shorter observation times. Soycan and Ata (2011) compared Global Positioning System (GPS)-only PPP solutions to Bernese software solutions achieving centimeter-level precision for durations exceeding 3 h. Gandolfi et al. (2017) conducted an analysis of PPP solutions focusing on short intervals and attained horizontal repeatability within 10 cm for datasets spanning half-an-hour durations. Barbarella et al. (2018) proposed an empirically based mathematical formula relating session duration to PPP accuracy. El-Shouny and Miky (2019) emphasized the time savings and reliable performance for sessions exceeding 2 h. Studies with small datasets have also been conducted by El-Mowafy (2011), Jamieson and Gillins (2018), Bulbul et al. (2021), and Bilgen et al. (2022).

Previous studies on the effects of session length have, in general, two main weaknesses. First, the datasets used in these analyses are small and may not be statistically representative of the actual outcomes for different durations. Also, studies with limited-size datasets cannot account for seasonal effects which can be observed if an entire year is analyzed. Second, all previous studies known to us focused on a particular latitudinal region, neglecting the effects on precision induced by GNSS orbit inclination (Swaszek et al. 2018). This study aims to address these omissions and explore the precision of geodetic-grade coordinates obtained using PPP. Our dataset comprises 365 days of 24-h GPS-only Receiver INdependent EXchange (RINEX) files for the year 2021 from 516 continuous GNSS stations across 13 networks. The study area was designed to include all possible latitude ranges from 90°N to 90°S. We achieved this wide latitude range by using data within the Americas, spanning longitudes 30°–130°W. The 24-h RINEX files were windowed into smaller, non-overlapping sessions of 1-, 2-, 3-, 4-, 6-, and 12-h which, together with the original 24-h observing sessions, were processed using the GPSPACE PPP software (https://github.com/CGS-GIS/GPSPACE). The results were then compared against each stations' reference coordinate derived from a daily modeled position from extended linear trajectory models as described by Bevis and Brown (2014) and Bevis et al. (2019). Notably, this study boasts a vastly larger dataset compared to previous studies, consisting of over 11 million sessions. Our results show that the dispersion (or scatter) as a function of latitude and session length in the horizontal and vertical components can be modeled using a power-law function. We obtained parameters for each latitude bin for the north, east, and up components of our PPP analysis and, additionally, also provided fits for the total horizontal component. We present these results so that they can be used to estimate the expected scatter, as a proxy for observation uncertainty in a PPP session, based on its duration and latitude of the station.

2 Methods

2.1 Dataset

We gathered a one-year dataset consisting of 24-h RINEX files for the year 2021. At least one year of data was assembled to capture any seasonal effects on the PPP results. Although these effects are not directly analyzed in our study, including an entire year accounts for known quasi-periodic effects observed in GNSS time series. The 24-h RINEX files were acquired from the GNSS RINEX file archive within the Division of Geodetic Science at The Ohio State University (OSU), which continuously collects and stores permanent GNSS data from around the world for various studies.

Stations were selected within the longitudinal range of 30°–130°W, covering all latitudes from 90°N to 90°S (SI, Figure S1). This region roughly encompasses most of Canada, the lower 48 states of the United States, Mexico, Central America, and the entirety of South America. This selection provides the largest north-south land mass distribution with GNSS data.

In total, the selection comprises 516 continuous stations distributed across 13 networks (SI, Table S1 for the network distribution). Station elevations in this dataset range from −31 to 3,735 m. Figure 1 shows a histogram with the number of stations as a function of latitude.

To assess PPP solutions for short-duration observation periods, the daily RINEX files were divided into smaller time windows using the GFZRNX software package (Nischan, 2016). For every station and each day, this approach resulted in the creation of twenty-four 1-h files, twelve 2-h files, eight 3-h files, six 4-h files, two 12-h files, and one 24-h file.

2.2 Calculating PPP solutions

Parallel.GAMIT (available at https://github.com/demiangomez/Parallel.GAMIT) is a powerful Python software package designed for parallel GNSS data processing, particularly for extensive regional or global networks. Parallel.GAMIT was specifically chosen for GPS data processing in this project due to its

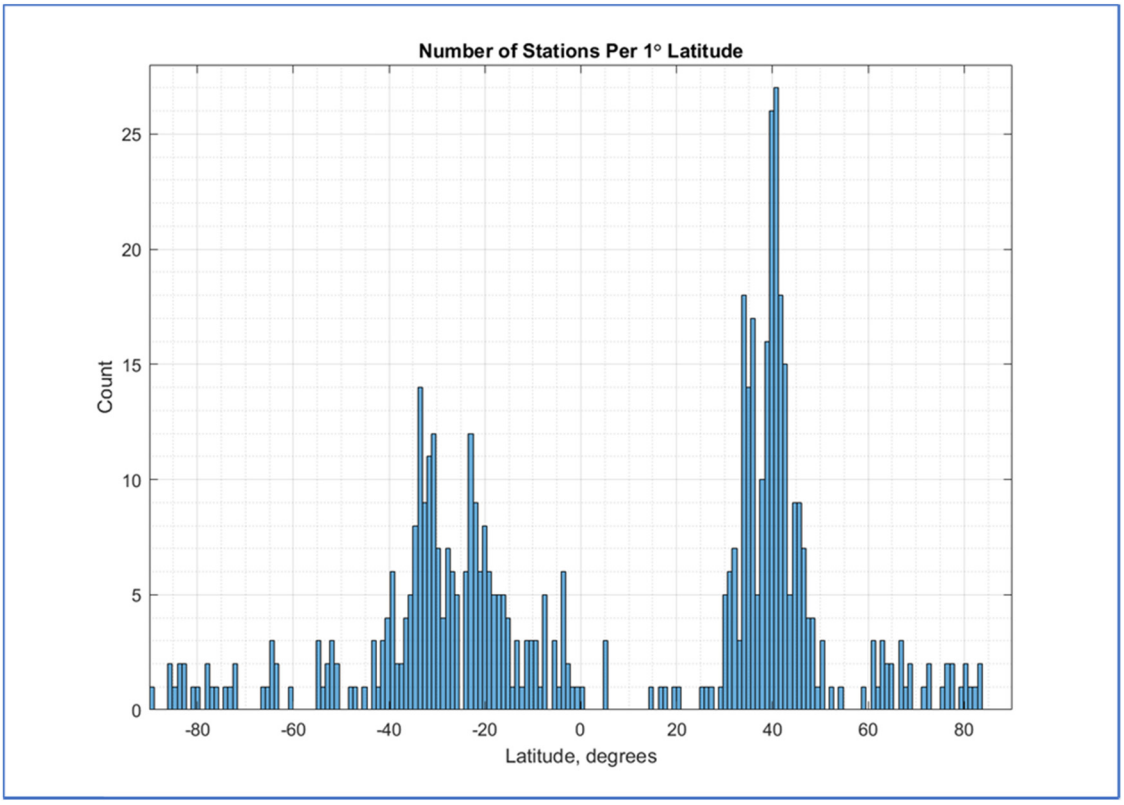

Figure 1: Station histogram as a function of latitude used in the study.

capacity to handle large datasets efficiently, thanks to its reliance on PostgreSQL (https://www.postgresql.org/) for maintaining data and metadata in a relational database. It consists of two main modules, namely, Parallel.GAMIT and Parallel.PPP. For the scope of this project, mainly the Parallel.PPP module was utilized.

Parallel.PPP serves as a Python wrapper for the former PPP software used by the Natural Resources Canada (NRCan) – Canadian Geodetic Survey (CGS), GPSPACE (Kouba and Héroux, 2001). This module is tailored to compute daily PPP solutions, which are subsequently used within Parallel.GAMIT. It's noteworthy that GPSPACE served as the underlying platform for the Canadian Spatial Reference System (CSRS)-PPP, one of the most widely used PPP services, until August 2018, at which point it was succeeded by a more modern package. Consequently, NRCan opted to release GPSPACE to the public, making it available to the broader community. Thus, GPSPACE continues to be used by many users around the world. Parallel.PPP leverages the capabilities of PostgresSQL for managing metadata, files, and directory tasks.

Although GPSPACE is able to process multi-GNSS data, our analysis used GPS-only data mainly to avoid biasing the results for stations that do not include multi-GNSS observations. Many stations used in this study have receivers that only record GPS, with only a few sites having full GNSS capabilities (especially in Latin America). Hence, using GNSS in our analysis would potentially bias the outcome (scatter) at stations without GNSS support. Yet, results using multi-GNSS would most likely reduce the scatter level. Therefore, the estimated precision of PPP solutions presented here can be considered an upper boundary relative to stations with the same sky view but observing more than one GNSS constellation.

For this project, Parallel.PPP carried out several key tasks, including collecting RINEX files from the OSU database, dividing the RINEX files into smaller windows using GFZRNX, calculating PPP solutions using GPSPACE, and determining the modeled true coordinates. Parallel.PPP was configured using IGS final orbits, the IGS14 reference frame, an elevation mask angle of 10°, and an observation interval of 30 s. RINEX files with smaller observation intervals were decimated to 30 s. We also applied ocean loading corrections using the FES2014b model (Lyard et al. 2021) and the Vienna Mapping Functions (Boehm et al. 2006) to estimate the zenith tropospheric delays, also noting that GPSPACE does not utilize integer ambiguity resolution techniques.

The execution of Parallel.GAMIT was carried out in parallel on a four-node Linux cluster, integrated into the

local high-performance computing environment known as Unity at OSU. In total, 11,009,920 out of 11,026,650 possible PPP solutions were solved for (equivalent to 99.8% of the dataset). The remaining 0.2% of the data presented some problem that precluded them from being processed. The typical processing time for each PPP solution was approximately 5.5 s. This time is equivalent to ~2 years of processing which, thanks to the parallel techniques employed here, only took 3 weeks using Parallel.GAMIT and Unity, representing a ~34× speedup.

2.3 Estimating the PPP scatter

The PPP solutions were transformed from their original Earth-centered Earth-fixed Cartesian coordinates to a local topocentric coordinate system in terms of easting, northing, and up relative to their reference coordinate, defined by the position of the station using the extended linear trajectory model (ELTM) from Bevis et al. (2019). An ELTM encapsulates a range of dynamic effects, including constant crustal motion, accelerating displacement patterns, abrupt shifts caused by seismic events and equipment changes, seasonal oscillations, and logarithmic transients following significant earthquakes. A full description of the use and capabilities of ELTMs can be found in the studies by Bevis and Brown (2014) and (Bevis et al., 2019). Using coordinates predicted by ELTMs avoids comparing data against a potentially noisy PPP solution, since the trajectory model of the station represents the best estimate for its long-term position using the entire data history. For reference, the average weighted root mean square error for a GNSS station trajectory is ~1 mm in the horizontal components and ~3 mm in the vertical. Additionally, using the ELTM coordinate allowed us to also provide dispersion estimates for the PPP 24-h session, since this coordinate is not directly used as a basis for comparison.

The results were analyzed in terms of their accuracy and precision. In this study, accuracy was characterized as the mean of the difference between the PPP-derived coordinates and each station's ELTM position. We analyzed the mean deviation of each station for the entire dataset (i.e. for the whole year that was processed) for the different PPP duration bins as a function of latitude. We found no significant bias relative to the ELTM solutions, and therefore, we focused on characterizing the scatter of each duration bin (Figure S2, SI). We also analyzed the correlation between the east and north scatter components of the dataset, and we found no significant correlation for each duration bin (as shown in Figure S3, SI).

For each station-duration bin pair, we computed the sample standard deviation for each coordinate thus

$$\sigma = \sqrt{\frac{\sum_{i=1}^{n}(x_i - \bar{x})^2}{n-1}}, \tag{1}$$

where σ represents the scatter around a station's position (obtained from its ELTM), n is the total number of observations in one bin, x_i is the ith observation in the dataset (east, north, and up), and $\bar{x}$ is the ELTM coordinate for the day being processed. Outliers within each time series were identified and removed using a threshold of three times the interquartile range. If an outlier was detected in either east, north, or up, the entire observation for all three components was discarded to avoid any biases in the standard deviation estimates. This process was applied across all duration bins and stations. Overall, 2.7% of observations were flagged and removed as outliers. The flagged outlier observation percentage is important because it provides an estimate of the probability of obtaining a solution that is significantly deviated from the statistics computed in this study. Table S2 in SI lists a complete list of removed outliers per duration.

3 Results

The effect of the GPS orbit configuration on dilution of precision (DOP) and, therefore, on the precision of a PPP solution has been already documented by other studies (e.g., Swaszek et al., 2018). To understand any latitude-dependent effects created by the GPS orbit configuration, we analyzed the dispersion dividing the data into latitude bins. Since we noticed, as expected, a symmetry between northern and southern latitudes, we grouped the stations based on their absolute value of latitude, with each bin separated by 10°. The size of the latitude bins was selected to maximize the resolution of the results and, at the same time, increase the number of stations per bin (so as to strengthen the statistics). We note, however, that wrapping the latitude about the geographic equator ignores some effects that are produced by ionospheric activity, which is approximately symmetric about the geomagnetic equator, which does not coincide with the geographic equator. Nevertheless, we analyzed the latitude-unwrapped results and found that our dataset did not include any significant signals that can be attributed to ionospheric activity. This might be, in part, since during the selected year of our analysis (2021) solar activity was not yet at its peak. Although the ionospheric effects are known to introduce noise in GPS solutions, isolating the ionospheric component of the scatter is outside the scope of our work.

We estimated the average standard deviation based on each station's individual standard deviation in the east, north, and up components within each latitudinal group and as a function of duration bin, as shown in Figure 2. We also obtained an overall horizontal deviation which was computed as the norm of the east and north components. This provides a measure of the expected overall standard deviation in the horizontal component, which might be a more practical measure of uncertainty for certain users. The midpoint of each latitude range (e.g., 5°, 15°, 25°..., 85°) serves as the representative value for each group.

As expected, longer observation sessions show lower levels of scatter, which are graphically represented in Figure 2. A few interesting observations can be made from these plots, especially for short-duration sessions. In the east component (Figure 2a), the scatter decreases for increasing latitudes, while in the north (Figure 2b), the scatter peaks at mid-latitudes to ~2.1 cm at 40°–50°. We attribute the observed behavior in the east scatter to the inability of a short PPP solution to correctly estimate the station's clock, which is more notably manifested in the east component scatter due to the Sagnac effect (Ashby,

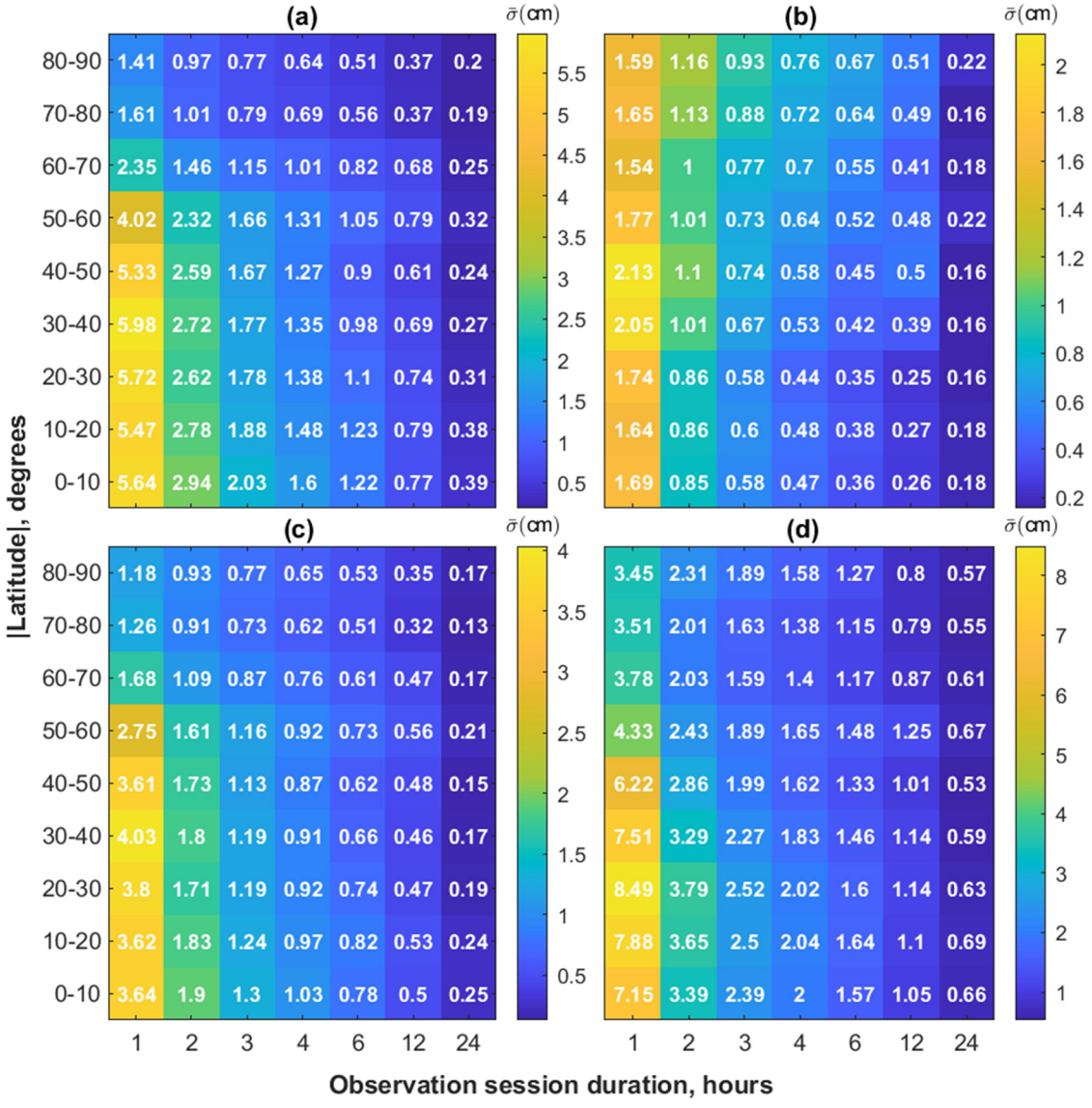

Figure 2: Average standard deviations of PPP solutions of continuous GPS stations grouped by duration and latitude range: (a) east component scatter for each latitude-session duration bin. Numbers in white represent the average scatter (in cm) for all stations within the bin; (b) same as (a) but for the north component; (c) same as (a) but for the horizontal component; and (d) same as (a) for the vertical component.

Table 1: The estimated parameters of the proposed function

$\lvert Lat_{min} \rvert$	$\lvert Lat_{max} \rvert$	East		North		Horizontal		Vertical	
		a	*b*	*a*	*b*	*a*	*b*	*a*	*b*
80	90	0.015	−0.598	0.017	−0.579	0.014	−0.601	0.035	−0.576
70	80	0.016	−0.638	0.018	−0.664	0.015	−0.688	0.032	−0.562
60	70	0.024	−0.631	0.016	−0.625	0.018	−0.656	0.032	−0.540
50	60	0.039	−0.745	0.016	−0.593	0.027	−0.746	0.038	−0.523
40	50	0.049	−0.924	0.018	−0.720	0.034	−0.919	0.050	−0.715
30	40	0.053	−0.913	0.017	−0.717	0.036	−0.937	0.059	−0.738
20	30	0.050	−0.857	0.014	−0.721	0.034	−0.882	0.068	−0.769
10	20	0.049	−0.793	0.014	−0.673	0.033	−0.801	0.064	−0.731
0	10	0.052	−0.809	0.014	−0.684	0.034	−0.817	0.059	−0.716

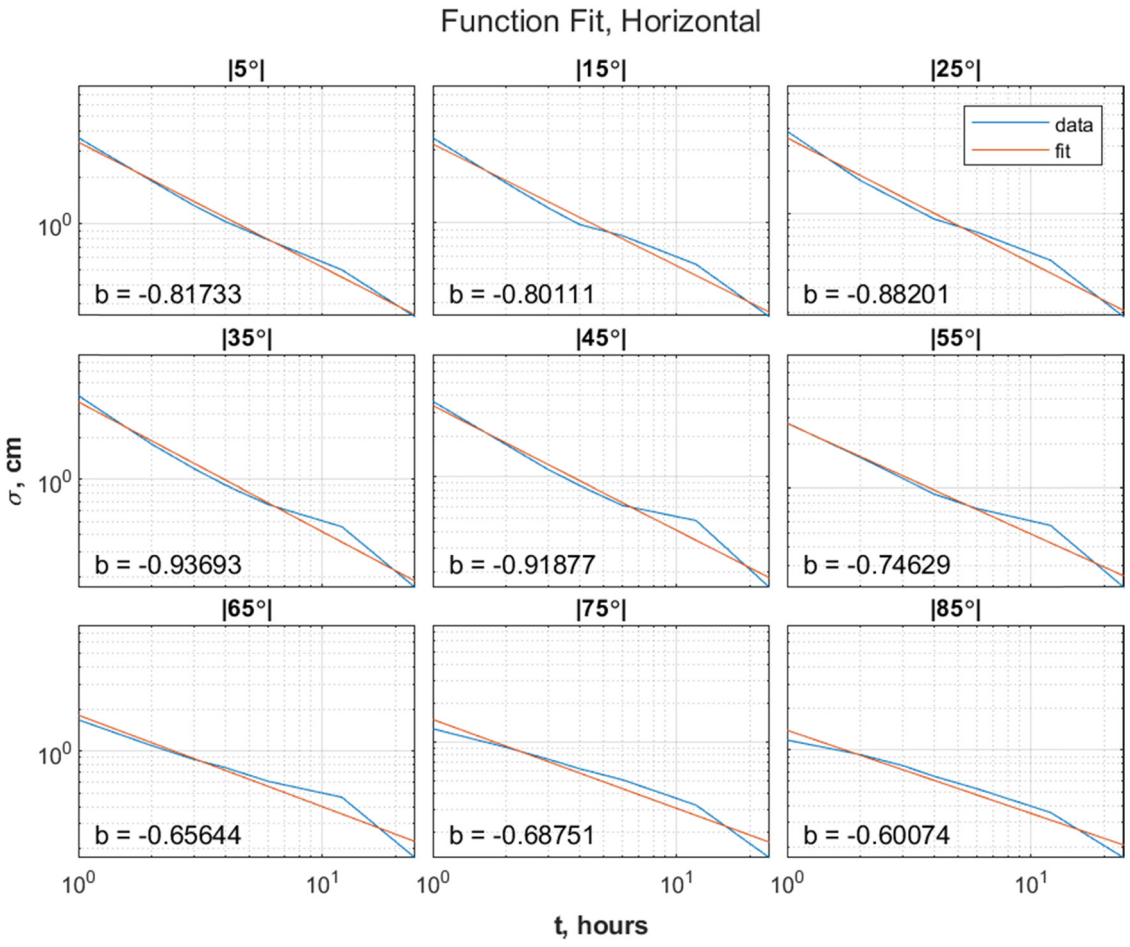

Figure 3: The observed scatter and power-law fits for the horizontal component. Each panel shows the central absolute latitude range with session duration in the *x*-axis (in h, log scale) and scatter in the *y*-axis (in cm, log scale). Blue line represents the data from Figure 2d and orange line the power-law fit.

2002). As session duration increases, this effect is reduced but it should be noticed that the scatter is uniform across all latitudes only in the 24-h session. Interestingly, the east component shows a sudden improvement in scatter at the 60°–70° bin in Figure 2a. We attribute this sudden improvement to the additional satellites appearing over the horizon on the northern or southern end of the satellites' sky-plots, which help constrain the station's clock

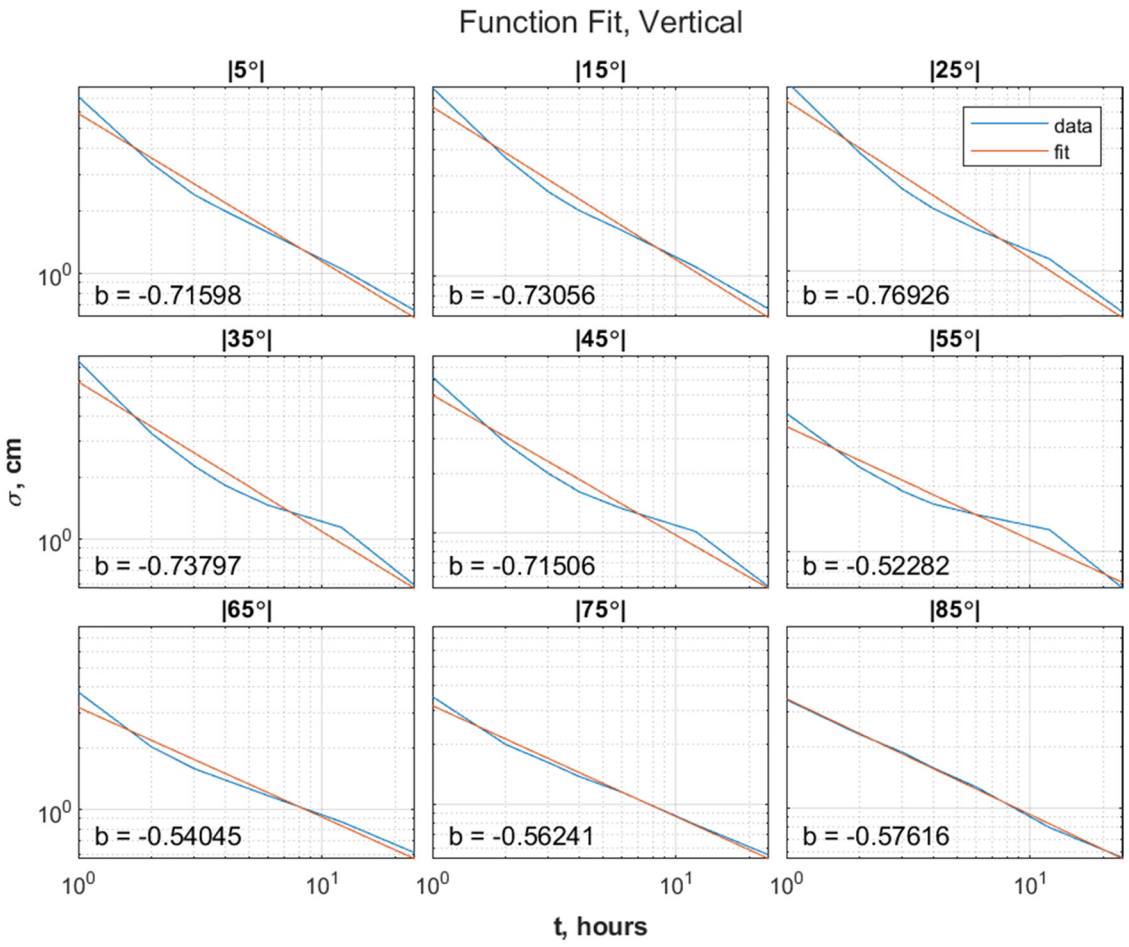

Figure 4: The observed scatter and power-law fits for the vertical component. Each panel shows the central absolute latitude range with session duration in the *x*-axis (in h, log scale) and scatter in the *y*-axis (in cm, log scale). Blue line represents the data from Figure 2d and orange line the power-law fit.

behavior for short sessions (similar to what is observed for the horizontal DOP in Figure 18 of Swaszek et al., 2018).

For the north component, we attribute the increased scatter at mid-latitudes to satellite orbit geometry which tends to create a "hole" in satellite sky plots in the north or south directions of the station (depending on which hemisphere the station is on). Nevertheless, this scatter represents about half of that in the east direction. The weak satellite coverage improves as latitude increases or decreases relative to a mid-latitude location (similar to what is observed in the east component around the 60°–70° bin). Moving towards the equator, the southern or northern satellite hole is significantly reduced. Moving towards the poles, the satellite hole tends to be closer to the zenith (or centered exactly at the zenith for stations at the geographic poles), allowing a station to observe satellites across all azimuth directions and thus improving the scatter in the north component. This increase in scatter is significantly reduced for sessions durations above 1 h. In the total horizontal component scatter (Figure 2c), it is clearly observed that the east component dominates over the north component scatter pattern.

For the vertical (Figure 2d), a surprising pattern emerges for 1 h duration sessions, where a larger scatter is observed at lower latitudes compared to high latitudes. This appears to contradict the orbit geometry (DOP) effect, previously discussed for the north component, which should worsen the vertical uncertainty at high latitudes, as described by Swaszek et al. (2018). Nevertheless, DOP estimates do not take into account that low-latitude stations are located in regions with higher water vapor content, while high-latitude regions are nearly always drier (Teng et al., 2013 – Figure 1). Water vapor is highly variable in space and time, and this heterogeneity makes the reliable estimation of delay parameters more difficult in humid areas. Figure 2d implies that the water vapor component has a stronger impact, in terms of scatter, than the geometric component.

To generalize the observed patterns across the east, north, and up components, we parameterized the average scatter shown in Figure 2. These parameterizations will allow us to directly calculate the expected scatter as a function of latitude and session duration. The next section discusses the proposed model for parameterizing the solution scatter for each latitude bin.

3.1 Parameterization

We introduce a model to describe the relationship between the precision of a PPP solution (σ) and the duration of the observation session (t), of the type,

$$\sigma = a \cdot t^{b}, \tag{2}$$

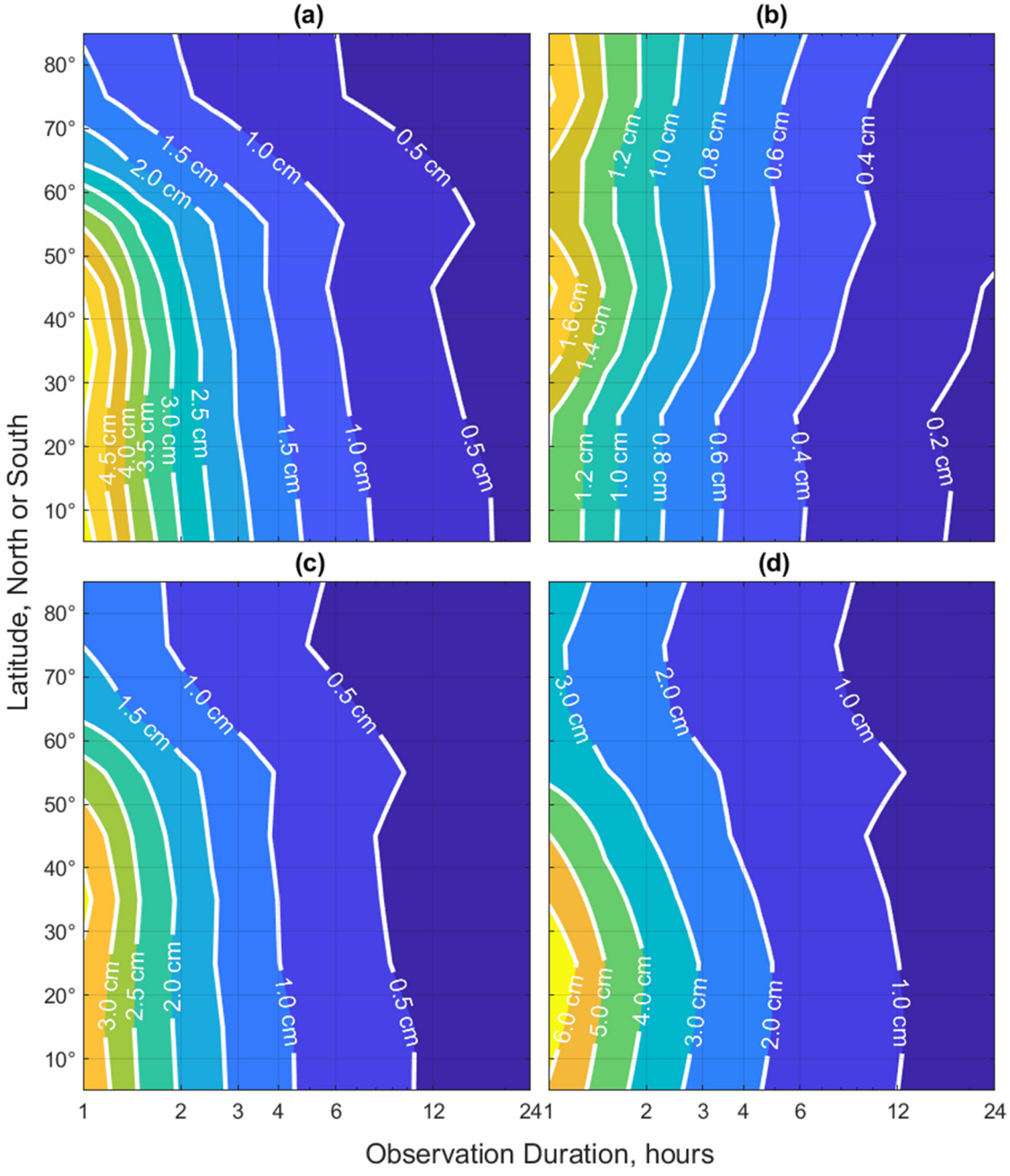

Figure 5: Expected precision of a PPP solution based on the duration and latitude of an observation as a continuous surface: (a) east, (b) north, (c) horizontal, and (d) vertical.

where parameters a and b are determined through a least squares optimization. To simplify the least squares procedure, we substitute $\alpha = e^a$ to linearize equation (2) as

$$\ln(\sigma) = \alpha + \ln(t)\cdot b. \quad (3)$$

This allowed us to employ the classical Gauss-Markov model to estimate the vector of unknown parameters, α and b. We note that while we can assign units to α (cm/h^b with b being dimensionless), this parameter does not represent a particular process other than the relationship between time and scatter. Hence, because these fits are purely kinematic, we don't assign specific units to a and directly assume that the output, σ, is in cm.

We performed the adjustment for each latitude-duration pair bin, as shown in Table 1, where we report the value of a *instead of* α. The observed scatter and their fits are shown for the horizontal in Figure 3 and for the vertical in Figure 4 (the east and north component fits can be found in the SI).

For clarity, the data were linearly interpolated in intervals of 30 min for occupation duration and one degree for latitude using the estimated parameters for each latitude bin. Contours at specific precisions were then overlaid onto the interpolated data. The final contour plot for all components being analyzed is shown in Figure 5.

4 Discussion

In this work, we estimated PPP solution uncertainties as a function of session duration. By including data that spans over the entire global latitude range, we also provide estimates of uncertainty as a function of station latitude. Furthermore, we adjusted a series of power-law parameters to each latitude bin (as a function of duration) to obtain a continuous estimate of uncertainty based on latitude and duration. Unsurprisingly, longer observation sessions reduce positioning errors, as shown in many previous studies. Our work, however, presents results that were obtained with several orders of magnitude more data than previous works. Our uncertainty estimates also include data for an entire year, which makes them more robust against potential seasonal effects in the northern and southern hemispheres. Therefore, our presented method provides an overall more robust estimate of PPP uncertainty as a function of the two main variables that affect the quality of a solution: session duration and latitude.

We also discussed the observed effects in precision as a function of latitude for a short session duration. We noted that positioning errors in the vertical tend to decrease with distance from the equator, as opposed to the DOP value which increases with latitude. This is somewhat surprising given that favorable conditions for satellite geometry decrease in this direction. We argue that this behavior is a result of the latitude dependence of total column atmospheric water vapor (Teng et al., 2013), which is known to affect the quality of GNSS solutions due to its high temporal variability. Further analysis correlating satellite availability, dilution of precision, and uncertainty as a function of time of the year could provide deeper insights into this and other effects. Given that results are GPS-only, potential increases in precision could be made by incorporating other constellations and integer ambiguity resolution PPP techniques which were not considered in the present work.

Because we used GPS observations from geodetic reference networks, the sky view at nearly every station was very good to excellent. Nevertheless, surveyors are often required to position points with much poorer sky view due to the presence of buildings, trees, or major topography. So, our model relating attainable positioning accuracy to station latitude and the time span of observations will provide only a lower bound on positioning error for stations with relatively poor sky view.

Acknowledgements: We thank Editor-in-Chief Mehdi Eshagh and two anonymous reviewers for their insightful comments which helped improve our work. We would also like to thank Keith Stewart and his Information Technologies team for their support of OSU's Unity cluster. This work acknowledges support from the School of Earth Sciences, The Ohio State University (Kurtz, Gómez, Bevis).

Author contributions: All authors contributed to the study's conception and design. BMK prepared the data and ran the programs to compute PPP locations. BMK performed the analysis with assistance from DDG and MGB. BMK wrote the first draft of the manuscript, and all authors commented on previous versions. All authors edited, commented, and approved the final manuscript.

Conflict of interest: Authors state no conflict of interest.

Ethics approval: Not applicable.

Consent to participate: Not applicable.

Data availability statement: Data is public and available through various websites, including the International GNSS Service data repository, the Argentine Instituto Geográfico Nacional, the Chilean Centro Sismológico Nacional, the

Instituto Brasileiro de Geografia e Estatística, and through the UNAVCO Facility Archive.

References

Ashby, N. 2002. "Relativity and the global positioning system." *Physics Today* 55, 41–7. doi: 10.1063/1.1485583.

Barbarella, M., S. Gandolfi, L. Poluzzi, and L. Tavasci. 2018. "Precision of PPP as a function of the observing-session duration." *IEEE Transactions on Aerospace and Electronic Systems* 54, 2827–36. doi: 10.1109/TAES.2018.2831098.

Bevis, M. and A. Brown. 2014. "Trajectory models and reference frames for crustal motion geodesy." *Journal of Geodesy* 88, 283–311. doi: 10.1007/s00190-013-0685-5.

Bevis, M., J. Bedford, and D. Caccamise II. 2019. "The art and science of trajectory modeling." In: *Geodetic time series analysis in earth sciences*, edited by J. P. Montillet, and M. Bos, pp. 1–28. Cham: Springer. doi: 10.1007/978-3-030-21718-1_1.

Bilgen, B., S. Bulbul, and C. Inal. 2022. "Statistical comparison on accuracies of web-based online PPP services." *Journal of Surveying Engineering* 148(4), 04022009. doi: 10.1061/(ASCE)SU.1943-5428.0000403.

Boehm, J., B. Werl, and H. Schuh. 2006. "Troposphere mapping functions for GPS and very long baseline interferometry from European Centre for Medium-Range Weather Forecasts operational analysis data." *Journal of Geophysical Research* 111. doi: 10.1029/2005JB003629.

Bulbul, S., B. Bilgen, and C. Inal. 2021. "The performance assessment of Precise Point Positioning (PPP) under various observation conditions." *Measurement* 171, 108780. doi: 10.1016/j.measurement.2020.108780.

El-Mowafy, A. 2011. "Analysis of web-based GNSS post-processing services for static and kinematic positioning using short data spans." *Survey Review* 43, 535–49. doi: 10.1179/003962611X13117748892074.

Gandolfi, S., L. Tavasci, and L. Poluzzi. 2017. "Study on GPS–PPP precision for short observation sessions." *GPS Solutions* 21, 887–96. doi: 10.1007/s10291-016-0575-4.

Ghoddousi-Fard, R and P. Dare. 2006. "Online GPS processing services: an initial study." *GPS Solutions* 10, 12–20. doi: 10.1007/s10291-005-0147-5.

Jamieson, M. and D. T. Gillins. 2018. "Comparative analysis of online static GNSS postprocessing services." *Journal of Surveying Engineering* 144, 05018002. doi: 10.1061/(ASCE)SU.1943-5428.0000256.

Kouba, J. and P. Héroux. 2001. "Precise point positioning using IGS orbit and clock products." *GPS Solutions* 5, 12–28. doi: 10.1007/PL00012883.

Kouba, J., F. Lahaye, and P. Tétreault. 2017. "Precise point positioning." In: *Springer handbook of global navigation satellite systems*, edited by P. J. G. Teunissen, and O. Montenbruck, pp. 723–51. Cham: Springer International Publishing.

Lyard, F. H., D. J. Allain, M. Cancet, L. Carrère, and N. Picot. 2021. "FES2014 global ocean tide atlas: design and performance." *Ocean Science* 17, 615–49. doi: 10.5194/os-17-615-2021.

Nischan, T. 2016. "GFZRNX – RINEX GNSS data conversion and manipulation toolbox." *GFZ Data Services*. doi: 10.5880/GFZ.1.1.2016.002.

Shouny, A. E. and Y. Miky. 2019. "Accuracy assessment of relative and precise point positioning online GPS processing services." *Journal of Applied Geodesy* 13, 215–27. doi: 10.1515/jag-2018-0046.

Soycan, M. and E. Ata. 2011. "Precise point positioning versus traditional solution for GNSS networks." *Scientific Research and Essays* 6, 799–808. doi: 10.5897/SRE10.799.

Swaszek P. F., R. J. Hartnett, K. C. Seals, J. D. Siciliano, and R. M. A. Swaszek. 2018. "Limits on GNSS performance at high latitudes." *Proceedings of the 2018 International Technical Meeting of The Institute of Navigation*, Reston, Virginia, January 2018, pp. 160–76.

Teng, W.-H., C.-Y. Huang, S.-P. Ho, Y.-H. Kuo, and X.-J. Zhou. 2013. "Characteristics of global precipitable water in ENSO events revealed by COSMIC measurements." *Journal of Geophysical Research: Atmospheres* 118, 8411–25. doi: 10.1002/jgrd.50371.

Tsakiri, M. 2008. "GPS processing using online services." *Journal of Surveying Engineering* 134, 115–25. doi: 10.1061/(ASCE)0733-9453(2008)134:4(115).

Zumberge, J. F., M. B. Heflin, D. C. Jefferson, M. M. Watkins, and F. H. Webb. 1997. "Precise point positioning for the efficient and robust analysis of GPS data from large networks." *Journal of Geophysical Research: Solid Earth* 102, 5005–17. doi: 10.1029/96JB03860.